HHS Public Access

Author manuscript

Oncogene. Author manuscript; available in PMC 2013 July 31.

Published in final edited form as:

Oncogene. 2013 January 31; 32(5): 577–588. doi:10.1038/onc.2012.84.

Synthetic lethality of Chk1 inhibition combined with p53 and/or p21 loss during a DNA damage response in normal and tumor cells

Sofia Origanti[1,2], **Shi-rong Cai**[1,2], **Amir Z. Munir**[1,2], **Lynn S. White**[1,2], and **Helen Piwnica-Worms**[1,2,3]

[1]Department of Cell Biology and Physiology, Washington University School of Medicine, Campus Box 8228, 660 S. Euclid Ave. St. Louis, MO 63110-1093, USA

[2]BRIGHT Institute, Washington University School of Medicine, Campus Box 8228, 660 S. Euclid Ave. St. Louis, MO 63110-1093, USA

[3]Department of Internal Medicine, Washington University School of Medicine, Campus Box 8228, 660 S. Euclid Ave. St. Louis, MO 63110-1093, USA

Abstract

Cell cycle checkpoints ensure genome integrity and are frequently compromised in human cancers. A therapeutic strategy being explored takes advantage of checkpoint defects in p53 deficient tumors in order to sensitize them to DNA damaging agents by eliminating Chk1-mediated checkpoint responses. Using mouse models, we demonstrated that p21 is a key determinant of how cells respond to the combination of DNA damage and Chk1 inhibition (combination therapy) in normal cells as well as in tumors. Loss of p21 sensitized normal cells to the combination therapy much more than did p53 loss and the enhanced lethality was partially blocked by CDK inhibition. In addition, basal pools of 21 (p53-independent) provided p53 null cells with protection from the combination therapy. Our results uncover a novel p53-independent function for p21 in protecting cells from the lethal effects of DNA damage followed by Chk1inhibition. Since p21 levels are low in a significant fraction of colorectal tumors, they are predicted to be particularly sensitive to the combination therapy. Results reported in this study support this prediction.

Keywords

cell cycle; checkpoints; apoptosis; cancer

*Corresponding author. Mailing address: Helen Piwnica-Worms, Ph.D., Department of Cell Biology and Physiology, Washington University School of Medicine, Box 8228, 660 South Euclid Ave., St. Louis, MO 63110. Phone: (314) 362-6812. Fax: (314) 362-3709. hpiwnica@wustl.edu.

Conflict of interest

The authors declare no conflict of interest.

Introduction

When exposed to DNA damaging agents, eukaryotic cells die, senesce or arrest their division cycles to allow time for DNA repair. The p53 and Chk1 proteins mediate cell cycle arrest in the G1-, S -and G2-phases of the cell division cycle under these conditions. p53 accomplishes this through transcriptional activation of downstream targets including p21 (1) whereas Chk1 promotes the ubiquitin-mediated proteolysis of the Cdc25A protein phosphatase (2–7). *TP53* is one of the most frequently mutated genes in human cancers and cells lacking a functional p53 pathway are unable to arrest in the G1 phase of the cell division cycle. p53 deficient tumor cells maintain their ability to arrest in the Sand G2-phases of the cell division cycle due to Chk1 activity. However, they are compromised in their ability to sustain these arrests (1). Importantly, Chk1 inhibitors selectively potentiate the cytotoxictiy of DNA damaging agents in tumor cells with nonfunctional p53 (8). Treating p53 deficient tumor cells with a DNA damaging agent or anti-metabolite followed by a Chk1 inhibitor causes tumor cells to move through the Sand G2-checkpoints with DNA damage and ultimately to die (9–13). Thus, combining Chk1 inhibitors with agents that induce genotoxic stress represents a therapeutic strategy to selectively target tumors with intrinsic checkpoint defects while minimizing toxicity in normal cells. Importantly, lowering Chk1 levels with Chk1-specific siRNAs, induces bypass of both the S- and G2-checkpoints in p53-deficient cells thereby phenocopying effects observed with Chk1 inhibitors (4). These studies validate Chk1 therapeutic target for treating p53-deficient tumors.

While performing studies to evaluate the dependency of p53 status on cellular responses to the therapies that combine DNA damage with Chk1 inhibitors, it became apparent that studies published to date relied on tumor cells cultured either ex vivo or as xenografts in rodents. Under these conditions, the individual contributions made by p53 mutation to experimental outcome cannot be directly assessed due to the plethora of additional uncharacterized mutations and genomic alterations present in these established cell lines. Furthermore, the transcriptional targets of p53 that protect cells from bypassing checkpoints in the presence of DNA damage and Chk1 inhibition have not been identified. p53 maintains checkpoint responses through transcriptional activation of several genes including p21, 14-3-3σ and Gadd45 (14). p21 loss has been reported in a majority of colon tumors (15) and silencing of 14-3-3σ by methylation has been reported in several cancers (16). Hence, it is important to determine how cells lacking p53 effectors respond to DNA damage coupled with Chk1 inhibition in order to understand which of these targets play dominant roles in locking down the cell cycle in the presence of DNA damage. To address these issues, we employed genetically defined mouse models (wild type, p53 null, p21 null and p53/p21 null mice) to assess whether DNA damage in combination with Chk1 inhibition selectively kills cells that are null for p53 but otherwise normal and to determine the role played by both basal and p53-induced pools of p21 in this process. Advantages of knock-out mouse models include the ability to study checkpoint control *in vivo* and the ability to circumvent mutational heterogeneity associated with tumor cells. Our studies identified p53 status as a key determinant of how cells with DNA damage respond to Chk1 inhibition and identified a role for p21, both basal- and p53 induced-pools, in protecting normal epithelial cells and colorectal tumors from the lethal effects of DNA damage as a single stress or in combination

with Chk1 inhibition. These results indicate that p21 attenuators may sensitize tumors, independent of their p53 status, to the lethal effects of DNA damage combined with Chk1 inhibition.

Results

DNA damage induced by irinotecan is independent of p53 status but enhanced by p21 loss

To specifically address the contribution made by p53 or p21 loss to the response of otherwise normal epithelial cells to the combination of DNA damage and Chk1 inhibition, wild type (WT) and p53 null mice were treated with vehicle (saline or DMSO); irinotecan (DNA damaging agent); UCN-01 (Chk1 inhibitor); or the combination of irinotecan and UCN-01. UCN-01 in combination with irinotecan is currently being tested in clinical trials in patients with advanced malignancies (8, 17). Irinotecan specifically damages S-phase cells by inducing single strand breaks that ultimately give rise to double strand breaks during the course of DNA replication. This leads to cell cycle arrest in the S- and G2-phases of the cell division cycle (18). Mice of 6 to 8 weeks of age were used as this is prior to the time when p53 null mice exhibit signs of lymphoma. We also focused on crypt epithelial cells of the small intestine owing to their rapid cell division cycles. Irinotecan treatment caused the accumulation of p53 (Fig. S1A) and p21 (Fig. S1B) in crypt epithelial cells of WT mice. Irinotecan also induced the accumulation of p53 in crypt epithelial cells of p21 null mice (Fig. S1A) and p21 accumulation was shown to be p53-dependent (Fig. S1B).

DNA damage was assessed by monitoring for phosphorylation of H2AX (γH2AX) since phosphorylation of this histone variant is one of the earliest events observed in cells with DNA double strand breaks (19). γH2AX staining was observed within the proliferating compartment of crypts (Fig. 1A) and at the base of the villi, which may represent differentiating progenitors that experienced DNA damage as they replicated in the crypt prior to their migration up into the villi (denoted by arrows in panel A). As seen in Fig. 1, γH2AX staining was not detected in vehicle-treated controls. In contrast, ~ 42% of cells stained positive for γH2AX in irinotecan-treated WT and p53 null mice. Even higher levels of DNA damage were observed in small intestinal epithelial cells of p21 null mice, with ~60% of cells staining positive for γH2AX.

Mice were also treated with UCN-01 alone or in combination with irinotecan and small intestines were isolated and analyzed for γH2AX. UCN-01 induced a mild DNA damage response in cells derived from WT and p53 null mice as ~ 2% of these cells stained positive for γH2AX. This DNA damage response was not unexpected, as partial loss of Chk1 has been shown to lead to DNA damage in other experimental settings (20). However, in p21 null cells the percentage of γH2AX positive cells increased to ~20% upon UCN-01 treatment. These data demonstrate that the ability of irinotecan or UCN-01, as single agents, to induce DNA damage in small intestinal epithelial cells is independent of p53 status but enhanced by p21 loss. The number of γH2AX positive cells was similar between cells treated with irinotecan alone or with irinotecan followed by UCN-01 (Fig. 1B).

Combination therapy induces apoptosis in p53- and p21-null cells

Next, the ability of the combination therapy to cause epithelial cells to undergo apoptosis was determined by examining small intestinal crypts for the presence of either cleaved caspase-3 (Fig. 2) or cleaved PARP (Fig. S1C). Apoptosis was not observed in crypt epithelial cells from vehicle-treated WT or p53 null animals. An occasional crypt epithelial cell was observed to undergo apoptosis in vehicle treated p21 null mice. Irinotecan induced apoptosis in ~1 cell per 2 crypts in mice that were WT for p53 (WT mice and p21 null mice) but not significantly in p53 null mice. As a single agent, UCN-01 did not induce apoptosis in WT or p53 null cells but a small number of p21 null cells were consistently observed to undergo apoptosis in vehicle and UCN-01 treated animals (Fig. 2B). Importantly, the combination therapy was able to induce apoptosis of p53 null cells and the effects were even more striking in p21 null cells. We also tested a second more selective Chk1 inhibitor, AZD7762 (13) for its ability to potentiate the effects of irinotecan in p53 and p21 null crypt epithelial cells. As seen in Fig. S1D, AZD7762 had some activity as a single agent but greatly enhanced the ability of irinotecan to induce crypt epithelial cells lacking either p53 or p21 to undergo apoptosis.

Bypass of DNA damage checkpoint in cells null for either p53 or p21

It has been proposed that DNA damage coupled with Chk1 inhibition induces cells to bypass DNA damage checkpoints resulting in mitotic catastrophe and cell death. Therefore, we monitored the ability of irinotecan to induce cell cycle arrest and UCN-01 to abrogate this arrest. Irintoecan was expected to arrest cells in the S and G2 phases of the cell division cycle thereby reducing BrdU incorporation and leading to higher levels of Geminin, a protein specifically expressed in the S- and G2-phases of the cell cycle (21). In addition levels of phosphorylated histone H3 (phistone H3) a mitotic marker (22, 23) were expected to be lower in cells with DNA damage due to G2 cell cycle arrest. Crypt epithelial cells of the small intestines have a high proliferative index in vehicle-treated animals, ~35–40% of cells stained positive for BrdU (Fig. S2) and Geminin (Fig. 3A). As expected, there was significant increase in the number of Geminin positive cells (Fig. 3A) as well as a significant decrease in both the number of BrdU positive (Fig. S2) and phistone H3 positive (Fig. 3B, C) cells in irinotecan-treated mice, indicative of cell cycle arrest. However, irinotecan was less effective at inducing cell cycle arrest in p21 null cells compared to WT and p53 null cells, as shown by the higher percentage of p21 null cells staining positive for BrdU (Fig. S2) and phistone H3 (Fig. 3B, C) in the presence of DNA damage. At baseline, there were 50% more p21 null cells that stained positive for phistone H3 compared with WT and p53 null cells (Fig. 3B, C). The higher mitotic index in intestinal epithelial cells lacking p21 indicates that p21 loss perturbs normal cell cycle regulatory circuits.

It was predicted that when UCN-01 was administered to irinotecan-treated animals, checkpoint bypass would be observed in p53 null but not p53 WT cells resulting in a reduction in Geminin staining coincident with an increase in phistone H3 staining. As seen in Fig. 3, checkpoint bypass was observed in p53 null but not WT cells. Interestingly, p21 null cells were even more sensitive than p53 null cells to the combination treatment as indicated by the higher numbers of phistone H3 staining cells (Fig. 3B, C).

We next asked whether there was a coincidence of checkpoint bypass and apoptosis in p53 null cells exposed to the combination therapy. This was accomplished by looking for crypt epithelial cells that co-stained for both phistone H3 and cleaved caspase-3 (Fig. S3A, B). ~ 2% of epithelial cells in crypts of p53 null mice and 8% in crypts of p21 null mice stained positive for both phistone H3 and cleaved caspase-3 indicating that these cells bypassed the G2 DNA damage checkpoint, entered into mitosis and engaged the apoptotic pathway (Fig. S3B). However, there were many more cleaved caspase 3 positive cells than phistone H3 positive cells, suggesting that either apoptosis occurred independent of checkpoint bypass in these cells or that the timing of organ harvest was not optimal to capture co-stained cells.

Cdk activation is required for combination therapy to induce checkpoint bypass and apoptosis

Next, the phosphorylation status of Cdk1/2 was examined in lysates prepared from the small intestines of treated animals (Fig. 4A). Tyrosine 15-phosphorylation (pY15) inhibits the enzymatic activity of Cdk1/2 (24) and therefore can be used to indirectly assess Cdk activity under a variety of conditions. As expected pY15 levels increased upon irinotecan-treatment in each genotype, indicative of Cdk inhibition in response to DNA damage (lanes 2, 6, 10) and Cdk1/2 became partially dephosphorylated on Y15 when mice were subsequently treated with UCN-01 (lanes 3, 7, 11). This was an expected result because UCN-01 inhibits Chk1 causing Cdc25A phosphatase levels to rise resulting in Cdk1/2 dephosphorylation (4). Although the combination treatment resulted in Cdk1/2 dephosphorylation in all cases, checkpoint bypass and apoptosis were only observed in crypt epithelial cells lacking p53 or p21 (Fig. 2, 3). Next, experiments were carried out to determine if Cdk activity is needed in order for the combination therapy to induce apoptosis (Fig. 4B, C). This was accomplished by treating mice with purvalanol A, a potent Cdk inhibitor (25). A reduction of the number of mitotic cells was observed in the small intestines of purvalanol A-treated mice demonstrating that the drug was bioavailable (Fig. S3C, D). Mice were subjected to the combination therapy followed by treatment with either vehicle or purvalanol A and small intestinal crypts were examined for cleaved caspase 3. There was a significant decrease (~50%) in the number of apoptotic (Fig. 4B, C) crypt epithelial cells in purvalanol A treated animals compared with vehicle treated controls. Thus, the combination treatment induced checkpoint bypass and apoptosis, at least in part, through Cdk activation.

Loss of p21 enhances combination treatment induced apoptosis in cells lacking p53

Crypt epithelial cells null for p21 but wild-type for p53 exhibited a robust apoptotic response to the combination therapy (Fig. 2) relative to p53 null cells that retained basal pools of p21. As expected, p21 was not induced by DNA damage in the absence of p53 (Fig S1B). The enhanced sensitivity of p21 null cells relative to p53 null cells to the combination therapy led us to ask if p53-independent (basal) pools of p21 played a role in protecting cells from the lethal effects of the combination therapy. To do this, double knockout mice lacking both p21 and p53 were treated with vehicle, irinotecan, UCN-01 or the combination therapy (Fig. 5 and Fig. S4A–C). Approximately 50% of vehicle-treated cells stained weakly for γH2AX indicating a significant amount of DNA damage in the absence of exogenous genotoxic and irinotecan treatment increased both the number and intensity of γH2AX positive cells (Fig. 5A, B and Fig. S4A, B). As expected, levels of tyrosine-phosphorylated

Cdk rose in cells of irinotecan-treated animals and fell in cells of mice treated with either UCN-01 alone or the combination therapy (Fig. 5C). These results demonstrated that the Chk1 pathway was active in these cells and the drugs were bioavailable in the small intestinal crypts of p53/p21 null animals. Similar to p21 null cells, irinotecan treatment did not significantly reduce BrdU incorporation (Fig. S4C, D) in p53/p21 double null cells, suggestive of intrinsic checkpoint defects in these cells. Importantly, the combination therapy induced checkpoint bypass in p53/p21 double null cells as evidenced by the increase in the number of mitotic cells observed in cells exposed to the combination treatment compared with cells exposed to irinotecan alone (Fig 5D, E). In addition, the combination therapy was capable of driving p53/p21 double null cells into apoptosis (Fig. 5F, G) but not to the same degree as that observed in cells null for p21 but WT for p53 (Fig. 2B). These results demonstrated that both p53-dependent and -independent mechanisms operate to induce apoptosis under these conditions and that p53-independent mechanisms were significantly enhanced in the absence of basal pools of p21. These results reinforce the conclusion that basal pools (p53 independent) of p21 provide a protective function in p53 null cells.

Loss of p21 enhances ability of combination therapy to drive p53 deficient colorectal tumor cells into apoptosis

Taken together, our results suggested that p21 deficient (p53 proficient) cells should be more susceptible to cell killing by combination therapies than p53-deficient (p21 proficient) cells. To test this and to determine the therapeutic efficacy of our findings, we employed an orthotopic colon cancer model whereby parental and mutant HCT116 tumor cells (1) were implanted directly into the cecum of immunocompromised mice as described previously (26). Prior to establishing the orthotopic xenografts, parental and p53 null HCT116 cells were transfected with plasmids expressing control (Ctrl) shRNAs or p21-specific shRNAs followed by selection in puromycin. Although HCT116 cells null for p21 have been reported (27), we detected endogenous p21 in these cells both at the protein and mRNA levels (data not shown). As seen in Fig. 6A, parental HCT116 cells transfected with Ctrl shRNAs maintained an intact p53 DNA damage signaling pathway as indicated by the accumulation of p53 and p21 upon UV-treatment. We were able to achieve knockdown (KD) of p21 in p53 null HCT116 cells (Fig. 6B, lane 3). Interestingly, when parental HCT116 cells (p53 WT) were knocked down for p21 and selected in puromycin, we observed a concurrent loss of p53 protein (Fig. S4E). This was not observed in parental HCT116 cells transiently transfected with plasmids encoding p21-specific shRNAs (Fig. S4F). Thus, p53 expression was selected against in HCT116 tumor cells lacking p21 function and as a result we were unable to obtain HCT116 cells that were WT for p53 but knocked down for p21.

Next, HCT116 cells (parental, p53 null and p53 null/p21 KD) were engineered to express a reporter gene encoding click beetle red luciferase, cells were implanted into the cecum of recipient mice and bioluminescence imaging was employed to demonstrate successful implantation of tumor cells (Fig. 6C). Mice were then exposed to either vehicle, irinotecan, AZD7762 (selective Chk1 inhibitor) or the combination of irinotecan and AZD7762. Tumors were removed and analyzed for phistone H3 (Fig. 6D) and cleaved caspase 3 (Fig. 6E, F). A significant increase in phistone H3 staining was observed in p53 null and p53

null/p21 KD cells compared to parental cells following exposure to the combination therapy. This indicates that cells deficient in p53 or both p53 and p21 bypassed the G2 DNA damage checkpoint. The combination therapy induced significantly more apoptosis in cells lacking both p53 and p21 compared with control and p53 null cells (Fig. 6E, F). Finally, p21 levels were restored in p53 null/p21 KD HCT116 cells, cells were implanted into the cecum of recipient mice and mice were treated as outlined above. As seen in Figure S5, restoration of p21 in p53 null/p21 KD cells significantly reduced their sensitivity to the combination therapy. These results validated the specificity of the p21-shRNA and confirmed that basal pools of p21 provide partial protection to p53-deficient tumor cells from the lethal effects of therapies that combine DNA damage with Chk1 inhibition.

Discussion

The development of anti-cancer regimens that take advantage of the molecular differences between normal and cancer cells is highly desirable. *TP53* is one of the most frequently mutated genes in human cancers and, as such, there is great interest in finding anti-cancer regimens that selectively target p53 deficient tumors. Importantly, Chk1 inhibitors such as UCN-01 and AZD7762 selectively potentiate the cytotoxicity of DNA damaging agents in tumor cells with nonfunctional p53 (11, 13, 28) and are currently being tested in several clinical trials (8). In our study, we circumvented the heterogeneity of transformed cells, and used mouse models to address the contribution made by loss of p53 and its effector p21 in sensitizing cells to the combination of DNA damage and Chk1 inhibition. Irinotecan as a single agent induced 10 fold more apoptosis of small intestinal epithelial cells in WT animals compared with cells from p53 null animals. This was in spite of the fact that levels of DNA damage induced by irinotecan were similar in WT and p53 null cells. Whereas irinotecan as a single agent was ineffective at driving p53 null cells into an apoptotic cell death, we found that treatment with Chk1 inhibitors was capable of enhancing apoptosis in response to irinotecan in these cells. This result unequivocally demonstrated that p53 is a significant determinant of how cells respond to DNA damage followed by Chk1 inhibition.

Intriguingly, crypt epithelial cells lacking p21 sustained more DNA damage than their WT or p53 null counterparts following exposure to irinotecan and were more susceptible to cell killing by the combination therapy. Given the large number of p53-regulated genes, it was not necessarily expected that the loss of a single target (p21) would have such a profound effect. These results demonstrated that Chk1 together with p53, largely through its downstream effector p21, protects crypt epithelial cells from the DNA damaging effects of irinotecan. In addition, this study demonstrates that p53-independent (basal) pools of p21, together with Chk1, protect crypt epithelial cells from the DNA damaging effects of irinotecan. Rodriguez et al. (2006) reported that HCT116 cells lacking p21 were sensitive to the combination of excess thymidine and Chk1 inhibition and they noted that p21 is induced when Chk1 is inhibited independent of p53 status. However, their study did not test the importance of p21 induction in p53 null cells by deleting it nor did they investigate the mechanism of cell death. Here we report the consequences of deleting p21 (in p53 null mice) and knocking down p21 (in p53 null tumor cells).

Our results demonstrated that basal pools of p21 (p53-independent) protected crypt epithelial cells from the DNA damaging effects of irinotecan as both p21 null and p21/p53 null cells exhibited higher levels of DNA damage following exposure to irinotecan than did cells from WT animals or cells from mice that were null for p53 but WT for p21 (Fig 1B, 5A). Despite similar levels of DNA damage, a higher fraction of crypt epithelial cells null for p21 (p53 WT) underwent apoptosis compared with crypt epithelial cells null for both p21 and p53. This suggests that tumors that are proficient in p53 signaling and have low levels of p21 will be the most susceptible to combination therapies that combine DNA damage with Chk1 inhibition due to their ability to induce p53-dependent and -independent forms of apoptosis. In addition, apoptosis observed in treated cells null for both p53 and p21 was higher than that that observed in treated cells null for p53 but WT for p21. Thus, combining p21 antagonists with the combination therapy (DNA damage and Chk1 inhbition) is expected to further sensitize p53 deficient tumors to the combination therapy.

p21 has many functions that might explain how p53-independent pools protect cells from the genotoxic effects of DNA damaging agents and Chk1 inhibitors. p21 inhibits cell cycle advancement by binding to and inhibiting CDKs (15). In addition to regulating cell cycle progression, p21 binds to proliferating cell nuclear antigen (PCNA), a DNA polymerase δ processivity factor, thereby blocking processive DNA synthesis (29). The cytoplasmic pool of p21 has been shown to regulate apoptosis by binding to and inhibiting the activity of proteins that induce apoptosis, including procaspase 3, caspases 8 and 10, and the protein kinases SAPK and ASK1 (30). Paradoxically, low levels of p21 promote assembly of cyclin D-CDK4/6 complexes and in this capacity has a positive role in promoting cell cycle advancement (31). In order to distinguish between the these diverse functions of p21 (Cdk regulator versus apoptotic regulator), we treated mice with the Cdk inhibitor purvalanol A. Results demonstrated that p21 exerts its protective effect, at least in part, through its ability to inhibit Cdk activation (Fig. 4C).

We also observed that crypt epithelial cells that were null for p53 but otherwise normal exhibited more modest apoptotic responses to the combination therapy than did p53 deficient cancer cells. In addition, experiments performed with a variety of cultured p53-deficient tumor cells have reported 50 to 100 fold more cell death with the combination therapy than with the DNA damaging alone (18, 32, 33). We measured a ~10 fold difference in the number of p53 null small intestinal epithelial cells undergoing apoptosis in response to the two treatment regimens. The differential response of non-transformed p53 mutant epithelial cells compared with transformed p53 mutant tumor cells to the combination therapy may be due to oncogenic stress present in p53 mutant tumor cells. Oncogenic stress activates the ATR/Chk1 pathway (34–36) and tumor cells depend on this signaling pathway to maintain some semblance of genome stability (37). HCT116 cells, used in this study, contain homozygous mutations in the mismatch repair gene *hMLH1* and this may also contribute to their sensitivity to the combination therapy. Thus, the differential response of p53 mutant *normal* cells versus p53 mutant *tumor* cells was likely due to the presence of additional mutations present in tumor cells that make them more vulnerable to cell death when subjected to DNA damage followed by Chk1 inhibition and points to the usefulness of this therapeutic strategy in treating cancers lacking a functional p53 pathway.

In conclusion, this study demonstrates that p21 status is a significant determinant of how cells with DNA damage respond to Chk1 inhibition and that p21 provides a protective effect in response to combination therapies, in both p53 proficient and deficient backgrounds. A major debilitating side effect of chemotherapy is GI-toxicity. Here we show that p21 protects intestinal epithelium from the toxicity associated with DNA damage and that Chk1 inhibition sensitizes p21 deficient tumors to DNA damaging agents. This is expected to provide a therapeutic window that facilitates killing of p21 deficient tumor cells while at the same time limiting G1 toxicity.

Materials and Methods

Additional information for the methods and materials used can be found in Supplemental Methods.

All animal experiments described in this study were carried out in strict accordance with the guidelines recommended for care and use of laboratory animals by the National Institutes of Health (NIH, USA). The Animal Studies Committee at Washington University (St. Louis) approved all animal protocols used in this study.

Genotyping *Trp53*, *Cdkn1a* [*p21*$^{WAF1/CIP1}$] mutant mice

Trp53 mutant mice (B6.129S2-*Trp53*$^{tm1T4j/J}$, stock # 002102) and *Cdkn1a* mutant mice (B6;129S2-*Cdkn1a*^{tm1Tyj}/J, stock# 003263) were obtained from The Jackson Laboratory. 6 to 8 week old *Trp53*$^{+/+}$*Cdkn1a* $^{+/+}$ (Wild type-WT), *Trp53*$^{-/-}$ littermates and *Cdkn1a* $^{-/-}$mice were used in this study. The *Trp53*$^{+/-}$ mutant mice and *Cdkn1a*$^{-/-}$ mice were bred to generate the double knockout mice (*Trp53*$^{-/-}$ *Cdkn1a*$^{-/-}$). 6–14 week old *Trp53*$^{-/-}$ *Cdkn1a*$^{-/-}$mice were used in this study.

Treatment regimen

Drugs and vehicles were administered to mice via an intraperitoneal (IP) route. Vehicle treated mice received 0.9% saline on Day 1; 24h later (Day 2) they received 30% dimethyl sulphoxide (DMSO) and were sacrificed 6h later. For single drug treatments, mice were injected with either 100 mg/kg irinotecan (Hospira, diluted in saline) and sacrificed 24h later, or 5 mg/kg UCN-01 (Sigma, dissolved in 30% DMSO) and sacrificed 6h later. For the combination treatment, mice were injected with 100 mg/kg irinotecan on Day 1; 24h later (Day 2) they received 5 mg/kg UCN-01 and were sacrificed 6h later. To inhibit Cdk1 *in vivo*, mice received 100 mg/kg irinotecan on Day 1; 24h later (Day 2) they were injected with 5 mg/kg UCN-01; 1h after receiving UCN-01, mice were injected with 68 mg/kg purvalanol A (Tocris) or vehicle (PEG400: DMSO 50:50) and sacrificed 5h later (Fig 4C). To ensure the bioavailability of purvalanol A and its ability to inhibit intestinal cell proliferation, animals were injected with two doses of the drug. 68 mg/kg purvalanol A or vehicle (PEG 400: DMSO 50:50) was injected followed by a second dose of purvalanol A (34 mg/kg) or vehicle 1.5h later and sacrificed 1h after the second dose (Fig S3C). The second dosing was administered because the half-life of purvalanol A in mice is ~1h (38). For AZD7762 treatment, mice received either 20 mg/kg AZD7762 (Axon Medchem) or vehicle (11.3% 2-hydroxypropyl-β-cyclodextrin diluted in saline) and were sacrificed 5h

later. For the combination treatment, mice were injected with 100 mg/kg irinotecan on Day 1, and 24h later (Day 2) they were injected with 20 mg/kg AZD7762 and sacrificed 5h later.

Immunohistochemistry (IHC) and immunofluorescence (IF)

All paraffin embedded intestinal sections were incubated with the following antibodies: serine139 phosphorylated H2AX (γH2AX, Cell Signaling Technology), Geminin (Santa Cruz), BrdU (Serotec), serine 28 phosphorylated histone H3 (Sigma-Aldrich), cleaved caspase-3 and cleaved PARP (Cell Signaling Technology). To assay for BrdU incorporation, mice were injected with BrdU (Amersham) according to the manufacturer's recommendations (2 ml per 100 g body weight) and sacrificed 30 min later.

Cell culture and transfection

Parental and p53 null HCT116 cells (human colon carcinoma cells) were transfected with a pcDNA plasmid expressing Click Beetle Red Luciferase (CBRluc) reporter linked to EGFP. Clones stably transfected with CBRluc-EGFP were selected by screening for zeocin (Invitrogen) resistance. CBRluc-EGFP expressing parental and p53 null HCT116 cells were transfected with pLKO.1 vector expressing either a p21 targeted shRNA or control shRNA directed against firefly luciferase (provided by the RNAi consortium of Broad institute and Children's discovery institute at Washington University). Stably transfected clones were selected by screening for puromycin (Invitrogen) resistance. To ensure stable knockdown, cells expressing p21 shRNA or control shRNA were screened by Western blotting.

Implantation and treatment of orthotopic colon tumors

For establishing orthotopic colon tumors, 1.3×10^6 cells were resuspended in 30 μl DMEM culture medium (GIBCO) and injected into the cecal wall of immunocompromised NOD/SCID gamma mice (The Jackson Laboratory, NOD.Cg-*Prkdcscid Il2rgtm1Wjl*/SzJ stock# 005557). Bioluminescence imaging was performed on days 3 and 7 post injection to monitor success of tumor implantation and growth. Bioluminescent images were acquired using the IVIS Lumina (Caliper). Images were analyzed using LivingImage software (Xenogen). Seven to nine days post implantation; mice were subjected to the following treatment schedule: t = 0h (Day 1) vehicle/irinotecan; t = 18h (Day 2) vehicle/AZD7762; t = 26h (Day 2) vehicle/AZD7762; t = 50h (Day 3) vehicle/irinotecan; t = 68h (Day 4) AZD7762/vehicle and mice were sacrificed at t = 73h (Day 4). The following drug doses were used: 100 mg/kg irinotecan and 25 mg/kg AZD7762. 0.9% saline and 11.3% 2-hydroxypropyl-β-cyclodextrin diluted in saline were used as the vehicle controls for irinotecan and AZD7762, respectively.

Microscopy

For IHC analysis, images were captured using an Olympus BX51 microscope carrying an Olympus DP-71 camera. Images were processed using DP-BSW software (Olympus). For analysis of IF staining, images were captured using an Olympus BX-61 microscope carrying a digital camera (C10600, Hamamatsu). Fluorescent images were processed using Microsuite Biological Suite analysis software (Olympus).

Western blotting

Intestines were isolated from treated mice and processed as described in supplemental methods. 150 μg of total protein from intestinal lysates were loaded in each lane and probed with the following antibodies: tubulin (1:1000, Sigma-Aldrich), p53 (1:500, Leica Microsystems), GAPDH (1:2000, Imgenex), p21 (F-5, 1:1000, Santa Cruz), phospho-Cdk1 Tyrosine 15 (1:750, Santa Cruz), and Cdk1-total (1:750, Santa Cruz). For Western blotting using HCT116 cell lysates, the following antibodies were used: p53 (sc-126, 1:1000, Santa Cruz), p21 (1:500, BD Biosciences,), tubulin (1:2500, Cell Signaling Technology), actin (1:6000, Sigma), GAPDH (1:4000, Imgenex).

Supplementary Material

Refer to Web version on PubMed Central for supplementary material.

Acknowledgments

We thank Dr. B. Vogelstein for providing the HCT116 cell lines. This study was supported in part by NIH GM047017, the KOMEN Foundation and P50 CA94056 to the Molecular Imaging Center at Washington University. H.P.-W. is a Research Professor of the American Cancer Society.

References

1. Bunz F, Dutriaux A, Lengauer C, Waldman T, Zhou S, Brown JP, et al. Requirement for p53 and p21 to sustain G2 arrest after DNA damage. Science. 1998; 282:1497–501. [PubMed: 9822382]
2. Shimuta K, Nakajo N, Uto K, Hayano Y, Okazaki K, Sagata N. Chk1 is activated transiently and targets Cdc25A for degradation at the *Xenopus* midblastula transition. EMBO J. 2002; 21(14):3694–703. [PubMed: 12110582]
3. Sorensen CS, Syluasen RG, Falck J, Schroeder T, Ronnstrand L, Khanna KK, et al. Chk1 regulates the S phase checkpoint by coupling the physiological turnover and ionizing radiation-induced accelerated proteolysis of Cdc25A. Cancer Cell. 2003; 3:247–58. [PubMed: 12676583]
4. Zhao H, Watkins JL, Piwnica-Worms H. Disruption of the checkpoint kinase 1/cell division cycle 25A pathway abrogates ionizing radiation-induced S and G2 checkpoints. Proc NatlAcad Sci USA. 2002; 99:14795–800.
5. Falck J, Mailand N, Syljuasen RG, Bartek J, Lukas J. The ATM-Chk2-Cdc25A checkpoint pathway guards against radioresistant DNA synthesis. Nature. 2001; 410:842–7. [PubMed: 11298456]
6. Goloudina A, Yamaguchi H, Chervyakova DB, Appella E, Fornace AJ Jr, Bulavin DV. Regulation of human Cdc25A stability by serine 75 phosphorylation is not sufficient to activate a S-phase checkpoint. Cell Cycle. 2003; 2:473–8. [PubMed: 12963847]
7. Hassepass I, Voit R, Hoffmann I. Phosphorylation at serine-75 is required for UV-mediated degradation of human Cdc25A phosphatase at the S-phase checkpoint. J Biol Chem. 2003; 278:29824–9. [PubMed: 12759351]
8. Ma CX, Janetka JW, Piwnica-Worms H. Death by releasing the breaks: CHK1 inhibitors as cancer therapeutics. Trends Mol Med. 2010; 17(2):88–96. Epub 2010/11/23. [PubMed: 21087899]
9. Bunch RT, Eastman A. Enhancement of cisplatin-induced cytotoxicity by 7-hydroxystaurosporine (UCN-01), a new G2 checkpoint inhibitor. Clin Cancer Res. 1996; 2:791–7. [PubMed: 9816232]
10. Wang O, Fan S, Eastman A, Worland PJ, Sausville EA, O'Conner PM. UCN-01: a Potent Abrogator of G2 Checkpoint Function in Cancer Cells With Disrupted p53. J Natl Cancer Inst. 1996; 88:956–65. [PubMed: 8667426]
11. Levesque AA, Eastman A. p53-based cancer therapies: Is defective p53 the Achilles heel of the tumor? Carcinogenesis. 2007; 28(1):13–20. [PubMed: 17088261]
12. Levesque AA, Fanous AA, Poh A, Eastman A. Defective p53 signaling in p53 wild-type tumors attenuates p21waf1 induction and cyclin B repression rendering them sensitive to Chk1 inhibitors

that abrogate DNA damage-induced S and G2 arrest. Mol Cancer Ther. 2008; 7(2):252–62. Epub 2008/02/19. [PubMed: 18281511]

13. Zabludoff SD, Deng C, Grondine MR, Sheehy AM, Ashwell S, Caleb BL, et al. AZD7762, a novel checkpoint kinase inhibitor, drives checkpoint abrogation and potentiates DNA-targeted therapies. Mol Cancer Ther. 2008; 7(9):2955–66. Epub 2008/09/16. [PubMed: 18790776]
14. Taylor WR, Stark GR. Regulation of the G2/M transition by p53. Oncogene. 2001; 20(15):1803–15. Epub 2001/04/21. [PubMed: 11313928]
15. Abbas T, Dutta A. p21 in cancer: intricate networks and multiple activities. Nat Rev Cancer. 2009; 9(6):400–14. Epub 2009/05/15. [PubMed: 19440234]
16. Ferguson AT, Evron E, Umbricht CB, Pandita TK, Chan TA, Hermeking H, et al. High frequency of hypermethylation at the 14-3-3 sigma locus leads to gene silencing in breast cancer. Proc Natl Acad Sci U S A. 2000; 97(11):6049–54. [PubMed: 10811911]
17. Fracasso PM, Williams KJ, Chen RC, Picus J, Ma CX, Ellis MJ, et al. A Phase 1 study of UCN-01 in combination with irinotecan in patients with resistant solid tumor malignancies. Cancer Chemother and Pharmacol. 2011; 67(6):1225–37. Epub 2010/08/10.
18. Kohn EA, Ruth ND, Brown MK, Livingstone M, Eastman A. Abrogation of the S phase DNA damage checkpoint results in S phase progression or premature mitosis depending on the concentration of 7-hydroxystaurosporine and the kinetics of Cdc25C activation. J Biol Chem. 2002; 277(29):26553–64. [PubMed: 11953432]
19. Sedelnikova OA, Pilch DR, Redon C, Bonner WM. Histone H2AX in DNA damage and repair. Cancer Biol Ther. 2003; 2(3):233–5. Epub 2003/07/25. [PubMed: 12878854]
20. Lam MH, Liu Q, Elledge SJ, Rosen JM. Chk1 is haploinsufficient for multiple functions critical to tumor suppression. Cancer Cell. 2004; 6(1):45–59. [PubMed: 15261141]
21. Perez RP, Lewis LD, Beelen AP, Olszanski AJ, Johnston N, Rhodes CH, et al. Modulation of cell cycle progression in human tumors: a pharmacokinetic and tumor molecular pharmacodynamic study of cisplatin plus the Chk1 inhibitor UCN-01 (NSC 638850). Clin Cancer Res. 2006; 12(23): 7079–85. [PubMed: 17145831]
22. Xu B, Kim S-T, Kastan MB. Involvement of Brca1 in S-phase and G2-phase Checkpoints after Ionizing Radiation. Mol Cell Biol. 2001; 21:3445–50. [PubMed: 11313470]
23. Tapia C, Kutzner H, Mentzel T, Savic S, Baumhoer D, Glatz K. Two mitosis-specific antibodies, MPM-2 and phospho-histone H3 (Ser28), allow rapid and precise determination of mitotic activity. Am J Surg Pathol. 2006; 30(1):83–9. [PubMed: 16330946]
24. Parker LL, Piwnica-Worms H. Inactivation of the p34cdc2-cyclin B complex by the human wee1 tyrosine kinase. Science. 1992; 257:1955–7. [PubMed: 1384126]
25. Goga A, Yang D, Tward AD, Morgan DO, Bishop JM. Inhibition of CDK1 as a potential therapy for tumors over-expressing MYC. Nat Med. 2007; 13(7):820–7. Epub 2007/06/26. [PubMed: 17589519]
26. Cespedes MV, Espina C, Garcia-Cabezas MA, Trias M, Boluda A, Gomez del Pulgar MT, et al. Orthotopic microinjection of human colon cancer cells in nude mice induces tumor foci in all clinically relevant metastatic sites. Am J Pathol. 2007; 170(3):1077–85. Epub 2007/02/27. [PubMed: 17322390]
27. Waldman T, Kinzler KW, Vogelstein B. p21 is necessary for the p53-mediated G1 arrest in human cancer cells. Cancer Res. 1995; 55(22):5187–90. [PubMed: 7585571]
28. Eastman A. Cell cycle checkpoints and their impact on anticancer therapeutic strategies. J Cell Biochem. 2004; 91(2):223–31. [PubMed: 14743382]
29. Luo Y, Hurwitz J, Massague J. Cell-cycle inhibition by independent CDK and PCNA binding domains in p21Cip1. Nature. 1995; 375(6527):159–61. Epub 1995/05/11. [PubMed: 7753174]
30. Besson A, Dowdy SF, Roberts JM. CDK inhibitors: cell cycle regulators and beyond. Dev Cell. 2008; 14(2):159–69. Epub 2008/02/13. [PubMed: 18267085]
31. Sherr CJ, Roberts JM. CDK inhibitors: positive and negative regulators of G1-phase progression. Genes Dev. 1999; 13(12):1501–12. Epub 1999/07/01. [PubMed: 10385618]
32. Kohn EA, Yoo CJ, Eastman A. The protein kinase C inhibitor Go6976 is a potent inhibitor of DNA damage-induced S and G2 cell cycle checkpoints. Cancer Res. 2003; 63(1):31–5. [PubMed: 12517773]

33. Tse AN, Rendahl KG, Sheikh T, Cheema H, Aardalen K, Embry M, et al. CHIR-124, a novel potent inhibitor of Chk1, potentiates the cytotoxicity of topoisomerase I poisons in vitro and in vivo. Clin Cancer Res. 2007; 13(2 Pt 1):591–602. Epub 2007/01/27. [PubMed: 17255282]

34. Fikaris AJ, Lewis AE, Abulaiti A, Tsygankova OM, Meinkoth JL. Ras triggers ataxia-telangiectasia-mutated and Rad-3-related activation and apoptosis through sustained mitogenic signaling. J Biol Chem. 2006; 281(46):34759–67. Epub 2006/09/14. [PubMed: 16968694]

35. Bartkova J, Rezaei N, Liontos M, Karakaidos P, Kletsas D, Issaeva N, et al. Oncogene-induced senescence is part of the tumorigenesis barrier imposed by DNA damage checkpoints. Nature. 2006; 444(7119):633–7. Epub 2006/12/01. [PubMed: 17136093]

36. Di Micco R, Fumagalli M, Cicalese A, Piccinin S, Gasparini P, Luise C, et al. Oncogene-induced senescence is a DNA damage response triggered by DNA hyper-replication. Nature. 2006; 444(7119):638–42. Epub 2006/12/01. [PubMed: 17136094]

37. Gilad O, Nabet BY, Ragland RL, Schoppy DW, Smith KD, Durham AC, et al. Combining ATR suppression with oncogenic Ras synergistically increases genomic instability, causing synthetic lethality or tumorigenesis in a dosage-dependent manner. Cancer Res. 2010; 70(23):9693–702. Epub 2010/11/26. [PubMed: 21098704]

38. Raynaud FI, Fischer PM, Nutley BP, Goddard PM, Lane DP, Workman P. Cassette dosing pharmacokinetics of a library of 2,6,9-trisubstituted purine cyclin-dependent kinase 2 inhibitors prepared by parallel synthesis. Mol Cancer Ther. 2004; 3(3):353–62. Epub 2004/03/18. [PubMed: 15026556]

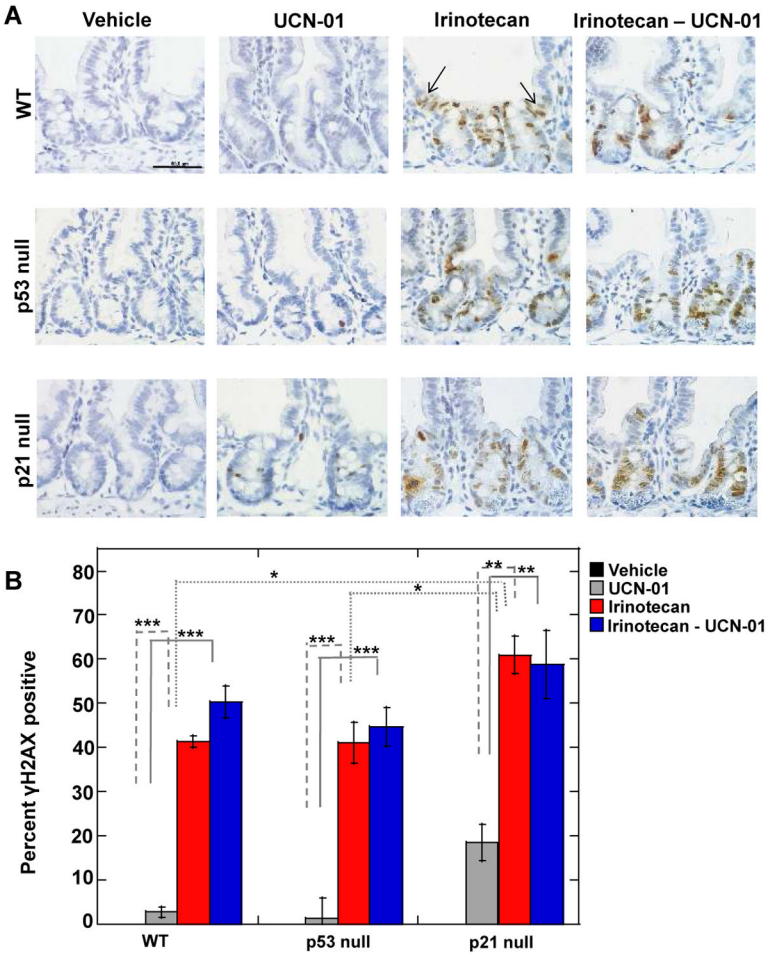

Figure 1. DNA damage induced by irinotecan is independent of p53 status but enhanced by p21 loss

(A) Small intestinal crypts isolated from wild-type (WT), p53 null and p21 null mice that had been subjected to the indicated treatments were examined by IHC for γH2AX (brown) and nuclei were counterstained with hematoxylin (blue). Scale bar =100 μM. Arrows indicate γH2AX positive cells that migrated up into the villi. (B) γH2AX positive nuclei were counted in images similar to those shown in panel A. Three mice were evaluated for each treatment group and a total of 250–400 crypt nuclei were scored per treatment group. Data are presented as mean +/− SEM. Asterisks indicate significantly different using one-way ANOVA. *p between 0.01 and 0.05; **p between 0.01 and 0.001; ***p< 0.001. Statistical significance for comparisons between irinotecan and the combination treatment across genotypes is indicated in Table S1.

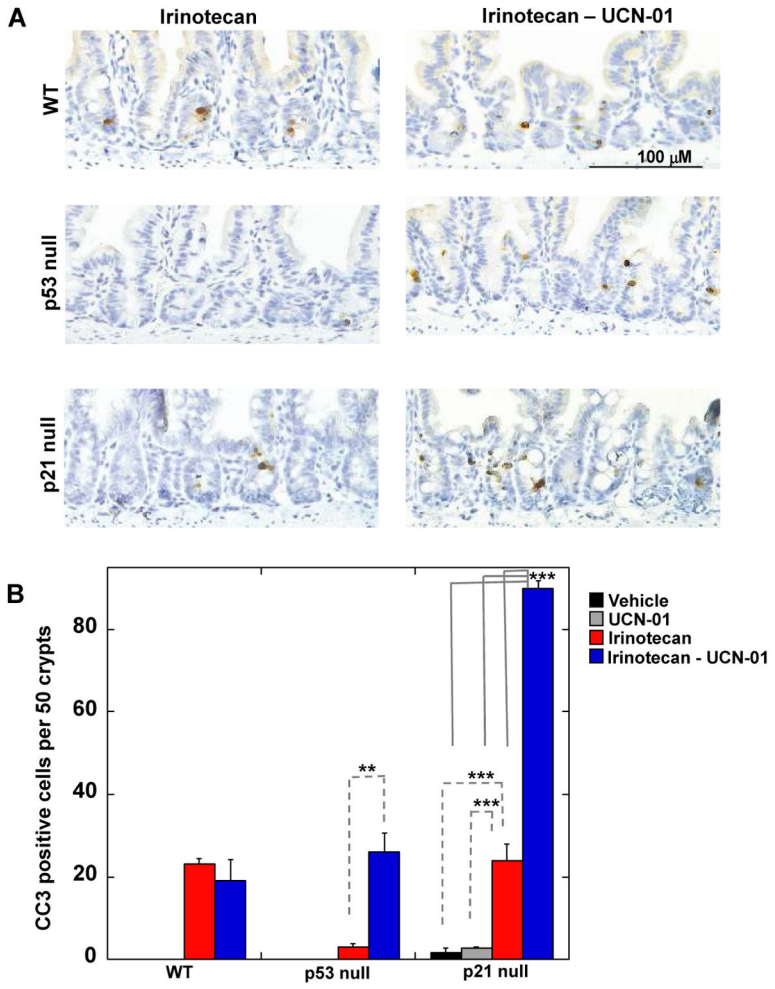

Figure 2. Loss of p53 or p21 sensitizes crypt epithelial cells to combination therapy

(A) Small intestinal crypts isolated from treated wild-type (WT) mice or mice null for either p53 or p21 were examined by IHC for cleaved caspase-3 (CC3) (brown) and nuclei were counterstained with hematoxylin (blue). Scale bar =100 μM. (B) The number of cells staining positive for CC3 was determined in a total of 50 crypts per treatment group (n = 3 to 5 mice per treatment group). Data are presented as mean +/− SEM. Asterisks indicate significantly different using a one way ANOVA. **p between 0.01 and 0.001, ***p < 0.001. Statistical significance for comparisons between irinotecan and the combination treatment across genotypes is indicated in Table S1.

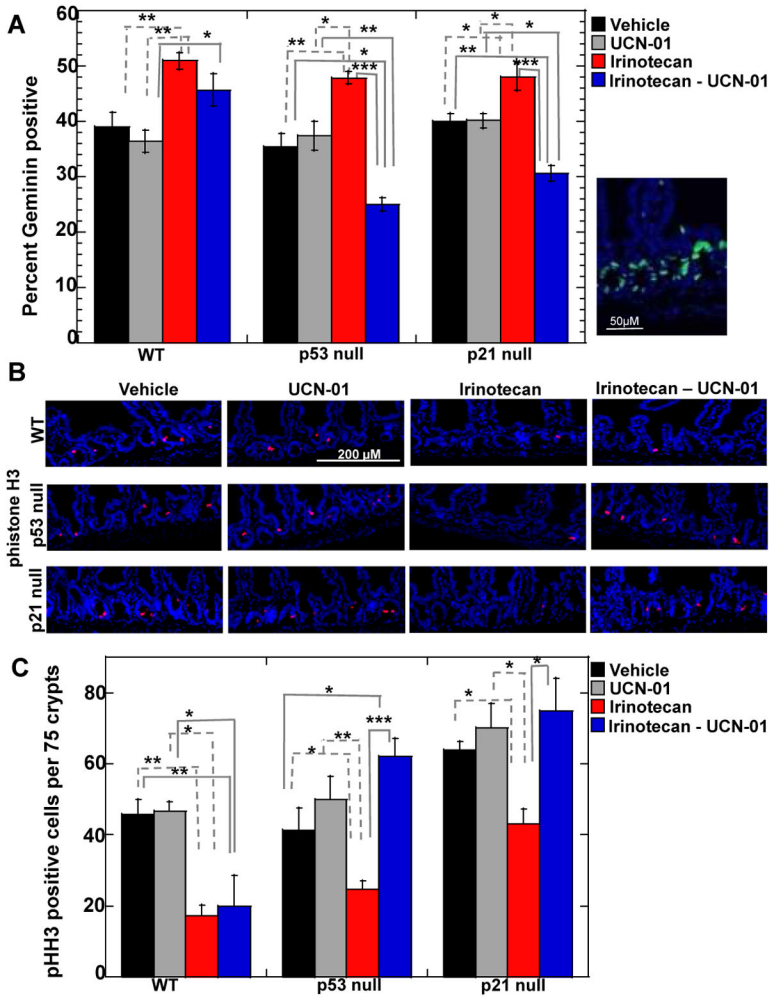

Figure 3. Combination treatment induces checkpoint bypass in crypt epithelial cells null for p53 or p21

(A) Small intestinal crypts isolated from treated wild-type (WT) mice or mice null for either p53 or p21 were examined for Geminin by immunofluorescent staining. Right panel illustrates Geminin positive cells in small intestinal crypts of irinotecan treated WT mice. Geminin (green); nuclei (blue, DAPI). Scale bar = 50 μM. Percentage of crypt epithelial cells staining positive for Geminin was determined by scoring 200 to 300 nuclei per mouse (n = 3 to 5 mice per treatment group). Data are presented as mean +/− SEM. Asterisks indicate significantly different as determined by a one-way ANOVA. *p between 0.01 and 0.05; **p between 0.01 and 0.001; ***p< 0.001. Significant difference was also observed between the combination treatments for WT compared to p53 null with p< 0.001and WT compared to p21 null with p< 0.001 (B) Small intestinal crypts isolated from treated mice were stained for phosphohistone H3 (pHH3) and the number of pHH3 positive cells per 75 crypts per mouse (n = 3 to 4 mice per treatment group) was determined (panel C). pHH3 (red); nuclei (blue, DAPI). Scale bar = 200 μM. Data are presented as mean +/− SEM. Asterisks indicate significantly different by a one-way ANOVA. *p between 0.01 and 0.05; **p between 0.01 and 0.001; ***p< 0.001. Statistical significance for pHH3 comparisons between irinotecan and the combination treatment across genotypes is indicated in Table S1.

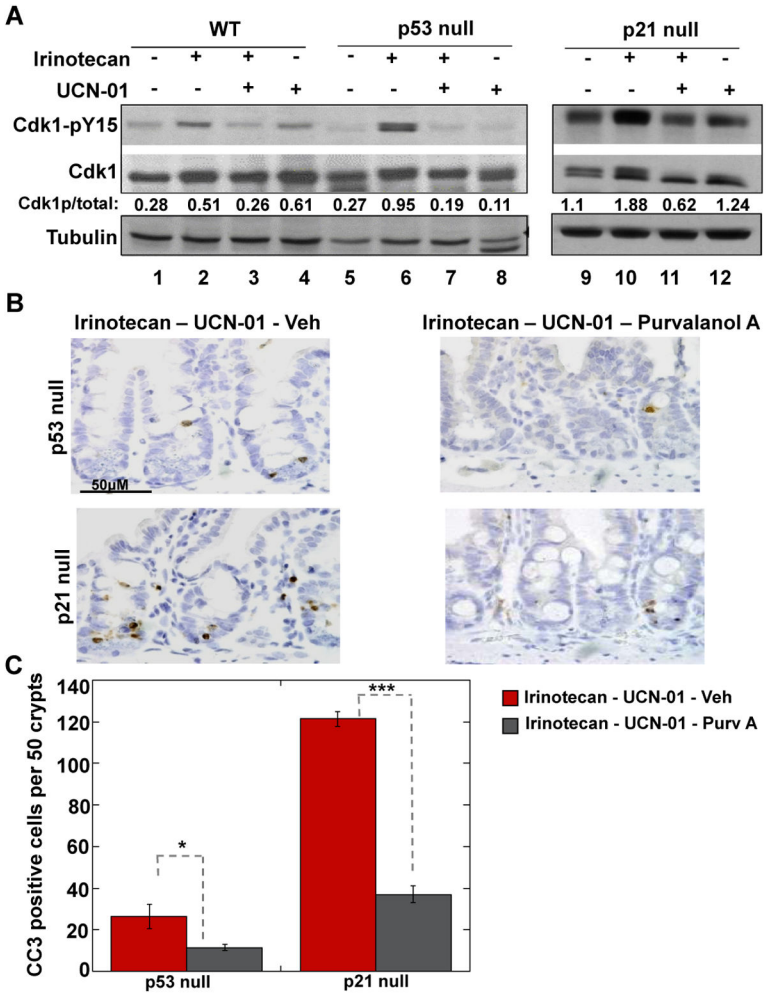

Figure 4. Effects of Cdk inhibition on ability of combination therapy to induce checkpoint bypass and apoptosis in crypt epithelial cells lacking p21 or p53

(A) Small intestines were isolated from treated WT mice (lanes 1–4), p53 null (lanes 5–8) and p21 null mice (lanes 9–12), and analyzed by Western blotting for Cdk1 (total levels), Cdk1 phosphorylated on tyrosine 15 (pY15) and tubulin. (B) Small intestinal crypts isolated from treated mice were examined for cleaved caspase-3 (CC3) (brown) and nuclei were counterstained with hematoxylin (blue) by IHC. Scale bar = 50 μM. (C) Cells staining positive for CC3 were counted in 50 crypts per mouse per treatment group (3 to 4 mice per treatment group). Data are presented as mean +/− SEM. Asterisks indicate significantly different using a two-tailed T-test. *p between 0.01 and 0.05, ***p < 0.001.

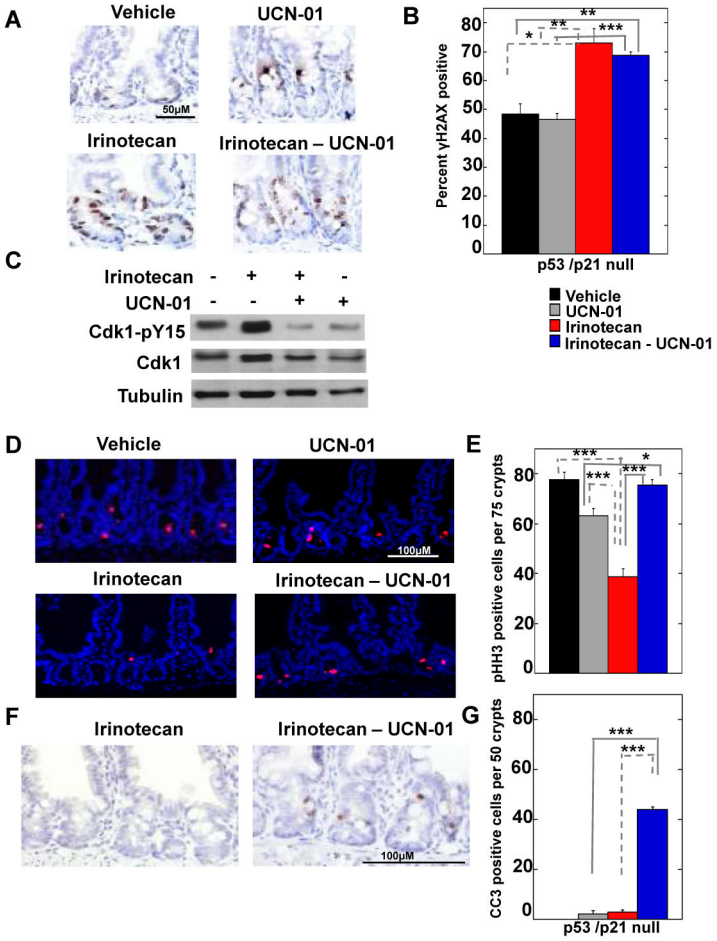

Figure 5. Basal levels of p21 levels protect small intestinal epithelial cells from lethal effects of combination therapy

(A) Small intestinal crypts isolated from treated mice null for both p53 and p21 were examined by IHC for γH2AX (brown) and nuclei (hematoxylin, blue). Scale bar = 50 μM. (B) Three mice were evaluated for each treatment group and a total of 150–200 crypt nuclei were scored for γH2AX positive nuclei in each treatment group. (C) Small intestines were isolated from treated mice and analyzed by Western blotting for Cdk1 (total levels), Cdk1 phosphorylated on tyrosine 15 (pY15) and tubulin. (D) Small intestinal crypts isolated from treated mice were stained for phistone H3 (pHH3, red) and nuclei (blue, DAP I) and (E) the number of pHH3 positive cells per 75 crypts was determined. Scale bar = 100 μM. Three mice were analyzed per treatment group. (F) Small intestinal crypts isolated from treated mice were examined for cleaved caspase-3 (CC3) (brown) and nuclei (hematoxylin, blue) by IHC. Scale bar = 100 μM. (G) The number of cells staining positive for CC3 was determined by counting CC3 positive cells in a total of 50 crypts per treatment group (n = 3 mice per treatment group). Data in panels B, E and G is presented as mean +/− SEM. Asterisks indicate significantly different by a one-way ANOVA.*p between 0.01 and 0.05; **p between 0.01 and 0.001; ***p< 0.001. Statistical significance for comparisons between irinotecan and the combination treatment across genotypes is indicated in supplementary Table S1.

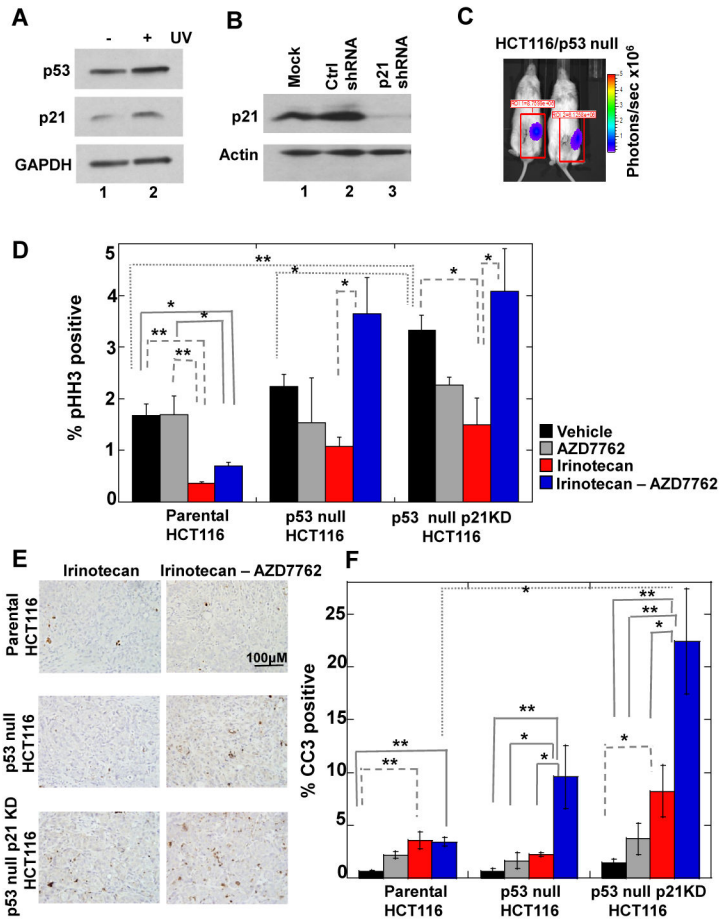

Figure 6. p53 null orthotopic colon tumors lacking basal p21 undergo profound cell death in response to combination therapy

(A) Parental HCT116 cells stably expressing click beetle red luciferase (CBRLuc) and control (Ctrl) shRNAs were either mock irradiated or exposed to 20 J/m^2 UV. Lysates were prepared and analyzed by Western blotting 24 h later. (B) Lysates prepared from p53 null HCT116 cells stably expressing CBRLuc and either Ctrl or p21 specific shRNAs were analyzed by Western blotting. (C) p53 null HCT116 cells stably expressing CBRLuc and Ctrl shRNAs were implanted into the cecum of immunocompromised mice. One week later, mice were injected with D-luciferin and subjected to bioluminescence imaging using the IVIS Lumina system (Caliper). Representative images of mice are shown. Photon flux is indicated by pseudocolored heatmap and tumor specific luciferase activity was measured by drawing a rectangular region of interest (ROI) as indicated (units: photons/sec × 10^6). (D) Treated mice engrafted with the indicated HCT116 cell lines were sacrificed and tumors were isolated and analyzed for pHH3 by immunofluorescence. Total and pHH3 positive cells were determined in three separate fields per tumor section per treatment group (n = 3 mice per treatment group). (E) Treated mice engrafted with the indicated HCT116 cell lines were sacrificed and tumors were isolated and analyzed by IHC for CC3 (brown) and nuclei were counterstained with hematoxylin (blue). (F) Total and CC3 positive cells were determined in four to five separate fields per tumor section per treatment group (n = 3 to 4 mice per treatment group). Scale bar =100 μM. Data in panels D and E is presented as mean

+/− SEM. Asterisks indicate significantly different by a one-way ANOVA. *p = 0.01 to 0.05, **p= 0.01 to 0.001.

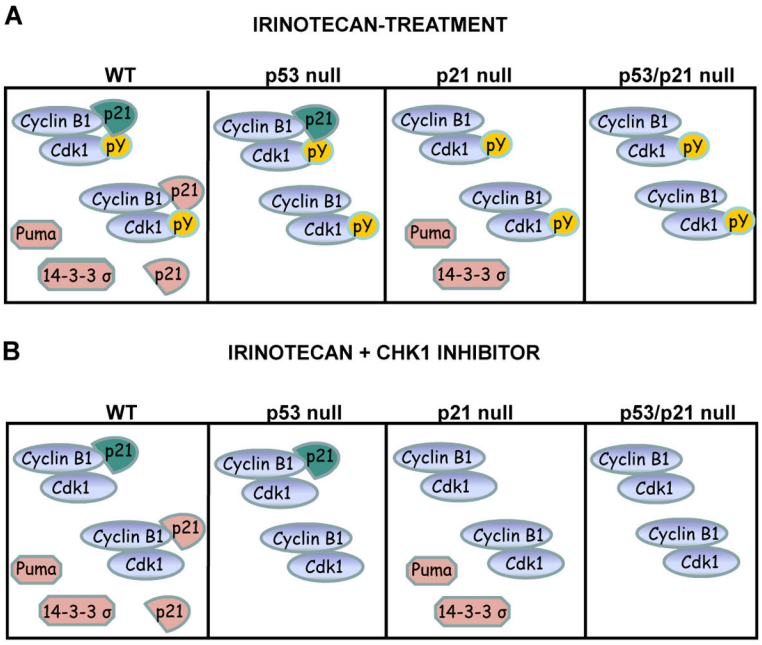

Figure 7. Model to explain the differential sensitivity of p53 and p21 null cells to DNA damage alone or combined with loss of Chk1 activity

(A) Small intestinal epithelial cells responded to irinotecan by activating a p53-dependent response pathway leading to the transcriptional activation of genes encoding cell cycle arrest (p21 and 14-3-3σ) and apoptotic (PUMA) proteins. Activation of cyclin-dependent protein kinases (Cdks) was prevented by at least two mechanisms including p21 binding and tyrosine phosphorylation (pY). Two pools of p21 were present in these cells (those that existed prior to irinotecan-treatment (basal or p53-independent, teal colored) and those that accumulated after irinotecan-treatment (p53-induced, salmon colored). Although equivalent levels of DNA damage were observed in p53 proficient and null cells, only p53 proficient cells underwent apoptosis, due to the accumulation of cell death proteins such as PUMA. In p21 null cells, DNA damage failed to efficiently inactivate Cdks due to loss of p21 (both p53-dependent and –independent pools) and cells did not efficiently arrest their cell division cycles under these conditions. Higher levels of DNA damage and therefore apoptosis (p53-dependent) were observed under these conditions. Cells lacking both p21 and p53 sustain high levels of DNA damage (due to loss of basal and induced pools of p21) but underwent less apoptosis (due to loss of p53-dependent apoptosis).

(B) Treating small intestinal epithelial cells with irinotecan followed by a Chk1 inhibitor, resulted in the tyrosine dephosphorylation of Cdks due to the accumulation of the Cdc25A phosphatase (4). However, both basal and induced p21 pools were able to maintain low Cdk activity under these conditions. Thus, Chk1 inhibition did not synergize with irinotecan to induce more DNA damage in normal intestinal epithelial cells. However, in p53 null cells treated with the combination therapy, loss of tyrosine phosphorylation coupled with loss of p21 synergized to induce apoptosis. Finally, levels of apoptosis were even higher in cells lacking p21 because these cells lack Cdk tyrosine phosphorylation as well as basal and induced pools of p21.